

UV-C Light Completely Blocks Aerosol Transmission of Highly Contagious SARS-CoV-2 Variants WA1 and Delta in Hamsters

Robert J. Fischer,* Julia R. Port, Myndi G. Holbrook, Kwe Claude Yinda, Martin Creusen, Jeroen ter Stege, Marc de Samber, and Vincent J. Munster



Cite This: *Environ. Sci. Technol.* 2022, 56, 12424–12430



Read Online

ACCESS |

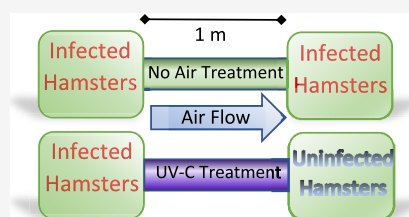
Metrics & More

Article Recommendations

Supporting Information

ABSTRACT: Behavioral and medical control measures have not been effective in containing the spread of SARS-CoV-2 in large part due to the unwillingness of populations to adhere to “best practices”. Ultraviolet light with wavelengths of between 200 and 280 nm (UV-C) and, in particular, germicidal ultraviolet light, which refers to wavelengths around 254 nm, have the potential to unobtrusively reduce the risk of SARS-CoV-2 transmission in enclosed spaces. We investigated the effectiveness of a strategy using UV-C light to prevent airborne transmission of the virus in a hamster model. Treatment of environmental air with 254 nm UV-C light prevented transmission of SARS-CoV-2 between individuals in a model using highly susceptible Syrian golden hamsters. The prevention of transmission of SARS-CoV-2 in a natural system by treating elements of the surrounding environment is one more weapon in the arsenal to combat COVID. The results presented indicate that coupling mitigation strategies utilizing UV-C light, along with current methods to reduce transmission risk, have the potential to allow a return to normal indoor activities.

KEYWORDS: SARS-CoV-2, COVID19, UV-C, transmission, aerosol, hamster



INTRODUCTION

The COVID-19 pandemic has officially caused more than 6.1 million deaths worldwide as of March 30, 2022.¹ Epidemiological and experimental data suggest that the primary mode of transmission of the virus is through airborne particles.^{2–5} Pharmaceutical countermeasures, such as vaccines and monoclonal antibody therapies, were rapidly developed but have had limited impact on controlling the pandemic. While the developed vaccines are highly effective against preventing severe COVID-19 and hospitalization, their transmission-blocking potential on the population level appears limited. Currently, 56% of the global population are fully vaccinated and an estimated 484 million people have been infected with SARS-CoV-2.¹ This has drastically changed the SARS-CoV-2 immune landscape and likely promoted the emergence of variants of concern (VoC) escaping antibody immunity, fueling the current global spikes in infection rates.⁶ These rapid spikes in SARS-CoV-2 prevalence prompt crude control measures such as travel restrictions, large-scale quarantining, and “lock downs” of entire populations, leading to economic and public health burden.⁷ The inability to control the ongoing SARS-CoV-2 pandemic has put the focus on the development of pathogen agnostic nonpharmaceutical intervention strategies.⁸ These nonpharmaceutical intervention strategies should ideally be practical, effective under multiple conditions, not depend on the cooperation of individuals, not be affected by or contribute to virus evolution, and prove efficacious for multiple pathogens with epidemic and pandemic potential. One measure that has the potential to decrease the concentration

of infectious airborne pathogens in enclosed spaces is ultraviolet (UV) light. Ultraviolet light, in particular UV-C light (wavelengths in the range of 200–280 nm), has germicidal properties and is effective in inactivating microorganisms such as fungi, bacteria, and viruses including SARS-CoV-2.⁹ UV-C light can be generated by highly efficient and well-established low-pressure (LP) mercury discharge lamps or UV-C light-emitting diodes that emit within the wavelengths of 250–280 nm.^{10–12} Specifically, the most optimal wavelengths for germicidal efficacy are around 254 nm and UV light at this wavelength is also known as germicidal ultraviolet (GUV) light.¹³ The mechanism of UV-C inactivation of viruses and bacteria is first a photochemical cross-linking reaction of nucleic acids, which prevents transcription and replication of RNA/DNA in host cells.¹⁴ A second photochemical reaction targets proteins, leading to protein molecular modifications, which can result in loss of host cell recognition of the virus and damage to membranes and envelopes.¹⁰ For a more comprehensive explanation of the inactivation of infectious pathogens with UV light, see the review by Katrina Browne.¹⁵

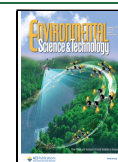
The ability of UV-C light to block transmission has been demonstrated in experiments where GUV light treated or

Received: April 20, 2022

Revised: August 11, 2022

Accepted: August 12, 2022

Published: August 24, 2022



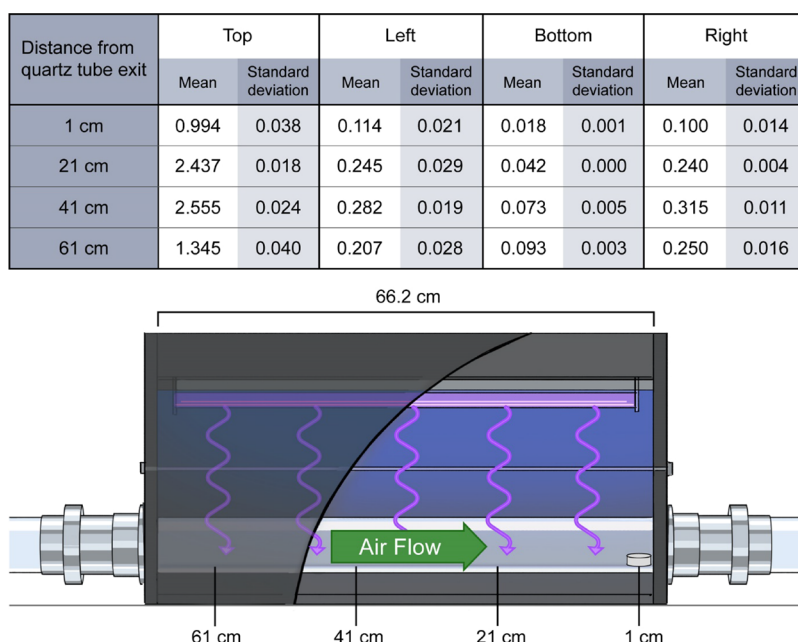


Figure 1. UV fluence measurements (mJ/cm^2). UV-C light incidence at 254 nm at four points along the length of the quartz tube at 20 cm intervals starting 1 cm from the UV-C containment box exit. Measurements were made with a UV-C meter type X1-1-UV-3725 measurement system, comprising a X1-5 optometer with a UV-3725-5 detector head, calibrated for narrow band sources such as LP mercury lamps. After a 1-hour lamp warmup, irradiance measurements (mW/cm^2) were taken in triplicate with the sensor facing (1) the UV-C light source (top), (2) away from the UV-C light source (bottom), (3) the right side of the box, and (4) the left side of the box. These irradiance dose measurements were used to calculate the total UV-C incidence dose (mJ/cm^2) along the length of the tube by multiplying irradiance dose by exposure time. The diagram shows the positions that the measurements were taken from and the placement of the sensor in the tube at 1 cm.

untreated air drawn from tuberculosis wards was the primary intake air in guinea pig air sampling enclosures.^{13,16} In trials where UV-C light was used to treat the upper layer of air in the treatment ward, 72–74% protection was conferred on the exposed guinea pig population compared to the trials where the air was not treated.^{13,16}

Several studies have shown that UV-C light can be used to inactivate coronaviruses, including SARS-CoV-2, on surfaces, in aqueous media, and even in aerosols using a UV-C germicidal lamp.^{17–21} Here, we report on the effectiveness of UV-C light in blocking transmission of airborne SARS-CoV-2 between individuals in a highly susceptible hamster model.

MATERIALS AND METHODS

Ethics Statement. All animal work was performed in an AAALAC International accredited facility, under animal study protocol # 2021-015 as approved by the RML Animal Care and Use Committee in accordance with guidelines set forth in the Guide for the Care and Use of Laboratory Animals 8th edition, the Animal Welfare Act, United States Department of Agriculture, and the United States Public Health Service Policy on the Humane Care and Use of Laboratory Animals.

The experiments were conducted in a BSL4 facility, and the samples were removed following approved SOPs.

Aerosol Transmission Apparatus. To determine if UV light is capable of arresting aerosol transmission between hamsters, we modified the aerosol transmission system described previously by Port et al.⁴ Two rodent boxes (Lab Products Inc.), one denoted as the donor box and the other the naïve box, were connected by a 1250 mm long by 73 mm inside diameter UV-C transparent quartz tube containing stainless-steel mesh at each end to prevent the hamsters from traversing the tube. The tube passed through a 662 mm long

high-density polyethylene (HDPE) box that housed the UV-C light source and shielded the surrounding area and animals from incident UV-C light. UV-C light was generated with two 58.7 cm Philips TUV F17T8 mercury lamps preaged to provide a stable UV-C light output. The center of the quartz tube was positioned at 205 mm from the UV-C source, 59 mm from the floor of the box, and 131 mm from the walls of the box.

A directional air flow, from the donor box to the naïve box, was created using a vacuum pump connected to the naïve box and controlled with a rotameter (King Instruments). Air entered the system through the filtered lid of the donor box, while the lid of the naïve box was fitted with an air impermeable film to ensure that the air flowed from the donor box to the naïve box.

Air was drawn through the system at 934.5 L/h representing approximately 30 air exchanges/h.

The velocity (v) of the air as it moves through the connecting tube was calculated by the following:

$$\frac{V_m}{A'_{\text{tube}}} = v \quad (1)$$

where V_m is the volume of air traveling through the connecting tube in cm^3/min and A'_{tube} represents the cross section of the connecting tube in cm^2 . The amount of time (t) needed for a front of air to traverse the tube was then calculated using

$$\frac{L}{v} = t \quad (2)$$

where L is the length of the tube in cm and v is the velocity in cm/min , calculated in eq 1.

The incidence of UV-C light at 254 nm was measured at four points along the length of the tube at 20 cm intervals

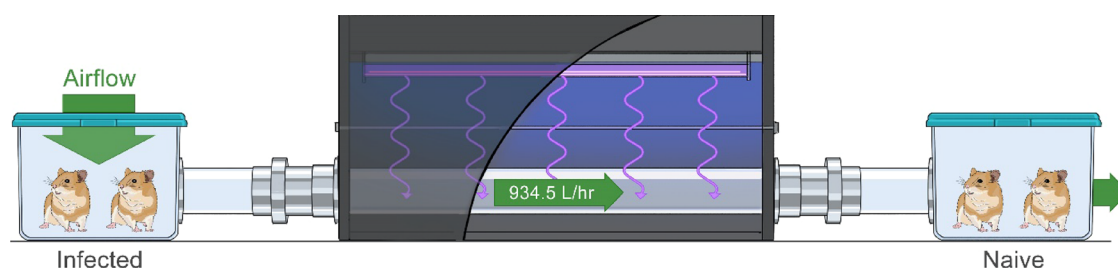


Figure 2. Experimental aerosol transmission with the UV-C irradiation setup. Two cages are separated with a 1250 mm \times 73 mm i.d. tube. The center portion of the tube is 662 mm of UV transparent quartz surrounded by a HDPE box housing a UV-C light source. Two donor hamsters, infected intranasally with 8×10^4 TCID₅₀ SARS-CoV-2 of either lineage A or the Delta variant 1 day prior to the experiment, were placed in the upstream cage, and two naive sentinel hamsters were placed in the downstream cage with a 934.5 L/h airflow for 4 h. The arrow indicates the direction of the airflow.

starting 1 cm from where the tube exits the UV-C containment box with a UV-C meter type X1-1-UV-3725 measurement system (Gigahertz-Optik Tuerkenfeld, Germany), comprising a X1-5 optometer with a UV-3725-5 detector head, calibrated for narrow band sources such as LP mercury lamps. After a 1-hour lamp warmup, irradiance measurements (mW/cm^2) were taken in triplicate with the sensor placed inside the tube facing (1) the UV-C light source (top), (2) away from the UV-C light source (bottom), (3) the right side of the box, and (4) the left side of the box (Figure 1). These irradiance dose measurements were used to calculate the total UV-C incidence dose (mJ/cm^2) along the length of the tube by multiplying irradiance dose by exposure time.

Total UV Incidence and UV-C Dose. To calculate the UV-C dose that pathogens traveling through the tube experience, an approximation was employed by using only the upward-registered irradiance values at the four measurement points. This simplification was used as these values are the main contributors. The resulting overall average dose is hence a minimal value. The upward facing UV-C irradiances at the four measurement points were plotted and a curve fitted to the points. The average UV-C irradiance was calculated by taking the integral from 0 to 66.2 cm (Supplemental Figure 1).

Cells and Virus. SARS-CoV-2 variant nCoV-WA1-2020 (Lineage A, EPI_ISL_404895) was obtained from Nathalie Thornburg at CDC. SARS-CoV-2 hCoV-19/USA/KY-CDC-2-4242084/2021 (Delta, B.1.617.2, EPI_ISL_1823618) was obtained from BEI resources. All virus stocks were sequenced, and no single nucleotide polymorphisms (SNPs) compared to the original patient sample sequence were detected. Virus propagation was performed in VeroE6 cells in Dulbecco's Modified Eagle Medium (DMEM) supplemented with 2% fetal bovine serum, 1 mM L-glutamine, 50 U/mL penicillin, and 50 $\mu\text{g}/\text{mL}$ streptomycin (DMEM2). To propagate the virus stock, 5 μL of virus stock was added to a T150 flask containing 20 mL of DMEM. Virus was harvested at the first signs of cytopathic effect (CPE), and the supernatant was collected and cleared of cellular debris by centrifuging at 1000 RCF. VeroE6 (a kind gift from Ralph Baric, UNC) cells were maintained in DMEM supplemented with 10% fetal bovine serum, 1 mM L-glutamine, 50 U/mL penicillin, and 50 $\mu\text{g}/\text{mL}$ streptomycin. No mycoplasma was detected in cells or virus stocks using the SouthernBiotech mycoplasma detection kit (SouthernBiotech, Birmingham, AL, USA).

Hamster-to-Hamster Transmission. Male and female Syrian golden hamsters 6 to 7 weeks old were used in these experiments. Sixteen hamsters were used for each experimental group. Hamster-to-hamster aerosol transmission was evaluated

using two donor hamsters and two naive hamsters for each of four replicates for every virus/condition. Donor hamster infections were carried out as previously reported.⁴ Briefly, 1 day prior to the experimental exposure, donor hamsters anesthetized via inhalation of vaporized isoflurane were inoculated intranasally with 8×10^4 TCID₅₀ SARS-CoV-2 Lineage A or the Delta variant.⁴ In the trials where UV-C was being used, the UV-C lamps were turned on 1 hour prior to the exposure to allow them to stabilize. To start the experiment, the naive animals were placed into their box, then the box was connected to the system, and the same was done for the donor animals. To start the experiment, the pump was turned on to produce an air flow from the donor cage to the naive cage. Based on previously published and unpublished data using a similar transmission caging system, we chose a set of conditions that we believed would provide a 100% infection rate in the non-UV-C group with a 4-hour exposure; therefore, the animals remained in the transmission system for 4 h, after which the exposed naive animals were singly housed in standard caging.⁴ The donor animals were anesthetized and then swabbed upon the completion of the 4-hour exposure, and the naive exposed animals were swabbed for 3 consecutive days starting on day 1 post exposure. On day 14, blood was drawn from the exposed naive animals for serology and the experiment was concluded.

RNA Extraction and Quantitative Reverse-Transcription Polymerase Chain Reaction. Oropharyngeal swabs were collected from anesthetized hamsters and placed in 1 mL of cell culture medium. RNA was extracted using a Qiagen viral RNA 96-well format kit on a Qiacube robot according to the manufacturer's instructions and following high containment laboratory protocols. qRT-PCR was carried out using a Taqman fast-virus 1-step master mix with previously described E_Sarbeco primers and probes (E gene) or sgLeadSARS2-F forward primers with E_Sarbeco reverse primers and probes (subgenomic E gene), on a Quant studio 3.²²

Enzyme-Linked Immunosorbent Assay (ELISA). ELISAs were performed as previously described.²² In brief, Maxisorp plates (Nunc) were coated with 50 ng of spike protein (Sinobiological SARS-CoV-2 (2019-nCoV) spike S1 + S2 ECD-HIS recombinant protein (catalog #40589-V08B1)) per well. Plates were incubated overnight at 4 $^{\circ}\text{C}$. Plates were blocked with Blocker casein in phosphate buffered saline (PBS) (ThermoFisher) for 1 h at room temperature (RT). Hamster serum collected on day 14 post exposure was diluted 1:400 in Blocker casein in PBS and incubated for 1 h at RT. Serum from a subset of positive qRT-PCR animals was titrated via a 2 \times serial dilution to obtain antibody titers of positive

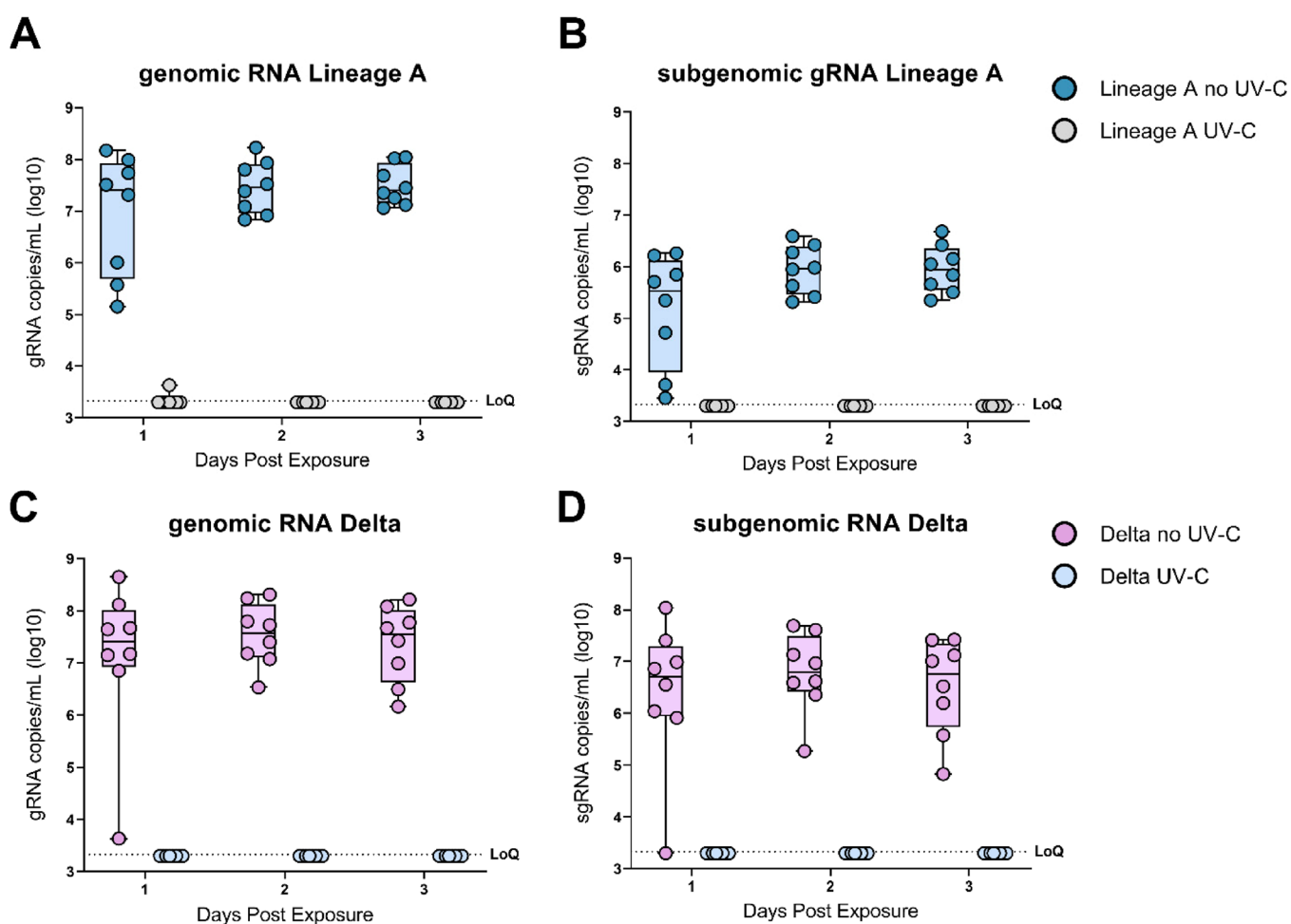


Figure 3. UV-C irradiation blocks SARS-CoV-2 aerosol transmission in hamsters. (A,B) Boxplot (minimum to maximum) of genomicRNA and subgenomicRNA Lineage A SARS-CoV-2 RNA in oropharyngeal swabs collected on 1-, 2-, and 3-days post exposure. Blue dots represent the no UV-C treatment group ($n = 8$), and gray dots represent the UV-C treatment group ($n = 8$). (C,D) Boxplot (minimum to maximum) of genomicRNA and subgenomicRNA Delta SARS-CoV-2 RNA in oropharyngeal swabs collected on 1-, 2-, and 3-days post exposure. Pink dots represent the no UV-C treatment group ($n = 8$), and light-blue dots represent the UV-C treatment group ($n = 8$). Dotted line = limit of detection.

animals. Secondary goat antihamster IgG Fc (horseradish peroxidase-conjugated, Abcam) spike-specific antibodies were used for detection and visualized with a KPL TMB 2-component peroxidase substrate kit (SeraCare, 5120-0047). The reaction was stopped with KPL stop solution (SeraCare), and the plates were read at 450 nm. The threshold for positivity was calculated as the average plus $3 \times$ the standard deviation of prebled serum from three animals as a negative control.

RESULTS AND DISCUSSION

To test the ability of UV-C light to prevent infection of naïve hamsters by naturally aspirated aerosols, we employed a modified version of an aerosol transmission system described previously.⁴ In this system, two cages are separated by a 1250 mm \times 73 mm tube resulting in a size exclusion of airborne particles $\geq 10 \mu\text{m}$. The central portion of the tube is quartz, enclosed in a HDPE box containing a UV-C light source (Figure 2). The length of the tube inside the box is 66.2 cm, and the air traveling from the infected animals to the naïve animals had a residence time of 10.7 s in the tube. A 934.5 L/h airflow, approximately 30 cage air exchanges per hour, is maintained throughout the experiment, resulting in a UV-C

dose exposure of the pathogen-containing airborne particles of approximately $21.4 \text{ mJ}/\text{cm}^2$.

Briefly, for each trial, two hamsters were inoculated intranasally with 8×10^4 TCID₅₀ SARS-CoV-2 strain nCoV-WA1-2020 (EPI_ISL_404895) (prototype lineage A SARS-CoV-2) or hCoV-19/USA/KY-CDC-2-4242084/2021 (EPI_ISL_1823618) (VoC Delta). At 1 day post infection (dpi), two infected hamsters were placed in the upstream (donor) cage and two naïve hamsters were placed in the downstream (naïve) cage. After a 4-hour exposure, the exposed naïve hamsters were moved to individual cages and the donor hamsters were euthanized after an oropharyngeal swab was collected.

To determine whether the naïve exposed sentinel hamsters became infected, oropharyngeal swabs were collected on days 1, 2, and 3 post exposure (DPE) and analyzed for the presence of subgenomic viral RNA (sgRNA, marker for active SARS-CoV-2 replication) and genomic viral RNA (gRNA) by qRT-PCR. The experiment was repeated 4 times for each of the following conditions: UV-C light treatment and no UV-C light treatment with variant nCoV-WA1-2020 or hCoV-19/USA/KY-CDC-2-4242084/2021 (Delta). When testing under UV-C conditions, the light was turned on 1 h prior to introducing the animals to the system.

All the animals in the no UV-C treatment groups had detectable viable virus as early as 1 DPE. gRNA was detected in all animals as early as 1 DPE for both lineage A and Delta VoC and continued through DPE 3 (Figure 3A,C). No gRNA was detected in either of the UV-C groups (Figure 3A,C). sgRNA was also detected on DPE 1–3 in the no UV-C treatment groups but not in any of the animals in the UV-C groups (Figure 3B,D). To additionally demonstrate the absence of transmission of SARS-CoV-2 in both UV-C treatment groups, the binding antibody titers against the SARS-CoV-2 spike protein (S) were determined on sera obtained at 14 DPE. To demonstrate that the donor animals were infected they were swabbed immediately after the exposure period concluded. The donor hamsters had viral loads from the swabs, based on the E gene, between \log_{10} 6.49 TCID₅₀/mL and 8.46 TCID₅₀/mL. A subset of no UV-C light treatment groups was tested and had high antibody titers ($\geq 52,000$ in all animals, $n = 8$), but both UV-C light treatment groups displayed a complete lack of binding antibody titers against SARS-CoV-2 S (< 400 in all animals, $n = 16$).

As the SARS-CoV-2 pandemic is well into its third year, additional nonpharmaceutical intervention strategies are urgently needed, especially in areas and locations where there is a higher risk of SARS-CoV-2 transmission, such as hospitals, COVID-19 testing centers, schools, and other indoor areas. Effective preemptive environmental intervention measures are instrumental in protecting health care workers and people at risk of developing severe COVID-19. The most widely promoted nonpharmaceutical countermeasures, such as mask wearing and social distancing, are highly dependent on compliance and as such have had varying levels of effectiveness across different cultural, political, and religious environments. These nonpharmaceutical interventions are based on the assumption that airborne respiration droplets are too large to pass through mask material or will settle to the ground within about 2 meters from the source. However, fine aerosols ($< 10 \mu\text{m}$) in diameter will remain suspended, floating on air currents for an extended amount of time, can travel more than 2 meters, and remain suspended for minutes to hours.²³

Although the dynamics of pathogen-laden airborne particles are more complicated than just large vs fine droplets, it is critical to determine the size of particles that most contribute to transmission.^{24,25} Respiratory droplets are emitted as a heterogeneous collection of various size particles traveling at a range of velocities depending on the mechanism of expulsion. Smaller particles tend to travel the farthest and remain suspended the longest. The disease state may change droplet composition and expulsion velocities.

Here, we were able to confirm the results of Bowen et al. and further demonstrate that a preemptive environmental intervention measure using UV-C irradiation can prevent the aerosol transmission of SARS-CoV-2 between hamsters.²⁶ This work suggests that UV-C could be used to decrease the concentration of viable air-borne virus in various environments used in conjunction with existing control measures and where other methods are less likely to work. Extensive literature is available for pathogen inactivation by UV-C treatment, using either bacterial spore inactivation tests, bacteria, or respiratory viruses.^{15,27} There are several UV-C systems that have been developed and are already being employed.^{28,29} The experiments described here are representative of air treatment in a ducted system. The efficiency of this type of system is dependent on the number of room-air exchanges per hour the

ventilation system processes. Typical comfort level ventilation systems handle between 1 and 2 room-air exchanges per hour.³⁰ The CDC recommends 6–12 air exchanges per hour for effective disinfection of room air.³¹ This exchange rate is not practical in many instances due to the cost involved in retrofitting and then maintaining ventilation systems and the noise associated with moving that volume of air. Another UV-C disinfection system that has been investigated is upper-room ultraviolet germicidal irradiation.³² Upper-room air ultraviolet germicidal irradiation utilizes UV-C lights located near the ceiling of a room and angled slightly upward in such a way that the occupants of the room are not exposed to any incident UV-C light.³³ In a study by McDevitt et al. investigating the decay rate of a poxvirus in a simulated hospital room, a single 25-watt UV-C unit, without any additional mixing, produced seven equivalent air changes per hour (eACH); when the test was repeated with vertical mixing from a simple ceiling fan, the effective rate was boosted to 92 eACH.³⁴ The same study investigated the effectiveness of UV-C to inactivate a poxvirus under steady-state conditions. Using four 25-watt lights, a 6 ACH mechanical ventilation system, and environmental conditions of 20 °C and 40% relative humidity (RH), they achieved an effective rate of approximately 1000 eACH.³⁴

The most compelling studies describing the effectiveness of upper-room air UV-C disinfection, however, were carried out in Peru and South Africa. These two studies demonstrated that upper-room UV-C is effective at reducing transmission of *Mycobacterium tuberculosis* from humans to guinea pigs in a clinical trial type of study. In these studies, UV-C treated or untreated air was exhausted from TB patients' rooms into animal holding rooms housing either 90 or 150 guinea pigs. Upper-room air UV-C treatment reduced infections by 80 and 70%, respectively.^{13,16} With statistical corrections, however, both studies achieved an approximate 80% reduction in infections.³⁰ It is worth noting that in these experiments, the UV-C light fixtures were mounted between 1.8 and 2.1 m high and that the room air was being exhausted at 1 m and “at breathing height”, respectively, so that the air being sampled was not drawn directly from the “kill zone”.

This study serves as additional proof of principle to promote further investigations into the use of GUV to reduce the risk of transmission in public spaces. This study is limited to demonstrating that GUV light can in fact block transmission. While beyond the scope of this study, additional studies are planned to determine the lowest effective dose needed to block transmission. These studies can be carried out using the system described here with some modification. To obtain actual dose response data, a known quantity of aerosolized virus would be introduced into the donor cage by fitting a collision nebulizer to the donor cage. UV filters can be applied to the UV chamber to regulate the amount of UV light reaching the virions passing through the quartz tube and the air reaching the naïve side assayed for viable virus. When breakthrough is achieved, naïve hamsters, as a more sensitive and biologically relevant detector, can be reintroduced into the system.

Preemptive environmental interventions that are not dependent on the compliance of the at-risk population would potentially be a highly cost-effective nonpharmaceutical countermeasure to help control the current pandemic. In addition, given the pathogen agnostic nature of UV-C germicidal irradiation, it has the potential to curb airborne transmission of fungal, bacterial, and viral pathogens, both life

threatening and common everyday maladies like the common cold.

■ ASSOCIATED CONTENT

SI Supporting Information

The Supporting Information is available free of charge at <https://pubs.acs.org/doi/10.1021/acs.est.2c02822>.

Graphical representation of UV incidence along the UV treatment zone (PDF)

■ AUTHOR INFORMATION

Corresponding Author

Robert J. Fischer – Laboratory of Virology, National Institute of Allergy and Infectious Diseases, National Institutes of Health, Hamilton, Montana 59840, United States;
orcid.org/0000-0002-1816-472X; Phone: (406) 363-9477; Email: fischerro@niaid.nih.gov

Authors

Julia R. Port – Laboratory of Virology, National Institute of Allergy and Infectious Diseases, National Institutes of Health, Hamilton, Montana 59840, United States

Myndi G. Holbrook – Laboratory of Virology, National Institute of Allergy and Infectious Diseases, National Institutes of Health, Hamilton, Montana 59840, United States

Kwe Claude Yinda – Laboratory of Virology, National Institute of Allergy and Infectious Diseases, National Institutes of Health, Hamilton, Montana 59840, United States

Martin Creusen – Signify, 5656 AE Eindhoven, The Netherlands

Jeroen ter Stege – UVConsult BV, 1611 AG Bovenkarspel, The Netherlands

Marc de Samber – Signify, 5656 AE Eindhoven, The Netherlands

Vincent J. Munster – Laboratory of Virology, National Institute of Allergy and Infectious Diseases, National Institutes of Health, Hamilton, Montana 59840, United States

Complete contact information is available at: <https://pubs.acs.org/doi/10.1021/acs.est.2c02822>

Funding

This work was supported by the Intramural Research Program of the National Institute of Allergy and Infectious Diseases (NIAID), National Institutes of Health (NIH) (1ZIAAI001179-01). Martin Creusen, Marc de Samber, and Jeroen ter Stege are affiliated with Signify N.V. and UVConsult BV and provided material support and expertise but no financial support.

Notes

The authors declare no competing financial interest.

■ ACKNOWLEDGMENTS

We would like to thank Neeltje van Doremalen, Jonathan Schulz, Emmie de Wit, Brandi Williamson, Natalie Thornburg, Bin Zhou, Sue Tong, Sujatha Rashid, Ranjan Mukul, Kimberly Stemple, Craig Martens, Kent Barbian, Stacey Ricklefs, Sarah Anzick, Rose Perry-Gottschalk, and the animal care takers for their assistance during the study and Maarten de Jager, Noud Fleuren, and Kevin Clark for their support in the design,

construction, and calibration of the UV-C apparatus. The following reagent was obtained through BEI Resources, NIAID, NIH: SARS-Related Coronavirus 2, Isolate hCoV-19/England/204820464/2020, NR282 54000, contributed by CDC.

■ REFERENCES

- (1) WHO. *WHO Coronavirus (COVID-19) Dashboard*, 2021.
- (2) Kutter, J. S.; de Meulder, D.; Bestebroer, T. M.; Lexmond, P.; Mulders, A.; Richard, M.; Fouchier, R. A. M.; Herfst, S. SARS-CoV and SARS-CoV-2 are transmitted through the air between ferrets over more than one meter distance. *Nat. Commun.* **2021**, *12*, 1653.
- (3) Zhang, R. Y.; Li, Y. X.; Zhang, A. N. L.; Wang, Y.; Molina, M. J. Identifying airborne transmission as the dominant route for the spread of COVID-19 (vol 117, pg 14857, 2020). *Proc. Natl. Acad. Sci. U. S. A.* **2020**, *117*, 25942–25943.
- (4) Port, J. R.; Yinda, C. K.; Avanzato, V. A.; Schulz, J. E.; Holbrook, M. G.; van Doremalen, N.; Shaia, C.; Fischer, R. J.; Munster, V. J. Increased small particle aerosol transmission of B.1.1.7 compared with SARS-CoV-2 lineage A in vivo. *Nat. Microbiol.* **2022**, *7*, 213–223.
- (5) Greenhalgh, T.; Jimenez, J. L.; Prather, K. A.; Tufekci, Z.; Fisman, D.; Schooley, R. Ten scientific reasons in support of airborne transmission of SARS-CoV-2. *Lancet* **2021**, *397*, 1603–1605.
- (6) Eguia, R. T.; Crawford, K. H. D.; Stevens-Ayers, T.; Kelnhofer-Millevolte, L.; Greninger, A. L.; Englund, J. A.; Boeckh, M. J.; Bloom, J. D. A human coronavirus evolves antigenically to escape antibody immunity. *PLoS Pathog.* **2021**, *17*, No. e1009453.
- (7) Tisdell, C. A. Economic, social and political issues raised by the COVID-19 pandemic. *Econ. Anal. Policy* **2020**, *68*, 17–28.
- (8) García de Abajo, F. J.; Hernández, R. J.; Kaminer, I.; Meyerhans, A.; Rosell-Llompart, J.; Sanchez-Elsner, T. Back to Normal: An Old Physics Route to Reduce SARS-CoV-2 Transmission in Indoor Spaces. *ACS Nano* **2020**, *14*, 7704–7713.
- (9) Biasin, M.; Bianco, A.; Pareschi, G.; Cavalleri, A.; Cavatorta, C.; Fenizia, C.; Galli, P.; Lessio, L.; Lualdi, M.; Tombetti, E.; Ambrosi, A.; Redaelli, E. M. A.; Saulle, I.; Trabattoni, D.; Zanutta, A.; Clerici, M. UV-C irradiation is highly effective in inactivating SARS-CoV-2 replication. *Sci. Rep.* **2021**, *11*, 6260.
- (10) Kowalski, W. *Ultraviolet Germicidal Irradiation Handbook*, 2009; pp 1–501.
- (11) Beck, S. E.; Ryu, H.; Boczek, L. A.; Cashdollar, J. L.; Jeanis, K. M.; Rosenblum, J. S.; Lawal, O. R.; Linden, K. G. Evaluating UV-C LED disinfection performance and investigating potential dual-wavelength synergy. *Water Res.* **2017**, *109*, 207–216.
- (12) Rattanakul, S.; Oguma, K. Inactivation kinetics and efficiencies of UV-LEDs against *Pseudomonas aeruginosa*, *Legionella pneumophila*, and surrogate microorganisms. *Water Res.* **2018**, *130*, 31–37.
- (13) Mphahlele, M.; Dharmadhikari, A. S.; Jensen, P. A.; Rudnick, S. N.; van Reenen, T. H.; Pagano, M. A.; Leuschner, W.; Sears, T. A.; Milonova, S. P.; van der Walt, M.; Stoltz, A. C.; Weyer, K.; Nardell, E. A. Institutional Tuberculosis Transmission Controlled Trial of Upper Room Ultraviolet Air Disinfection: A Basis for New Dosing Guidelines. *Am. J. Respir. Crit. Care Med.* **2015**, *192*, 477–484.
- (14) Cutler, T. D.; Zimmerman, J. J. Ultraviolet irradiation and the mechanisms underlying its inactivation of infectious agents. *Anim. Health Res. Rev.* **2011**, *12*, 15–23.
- (15) Browne, K. Brought to Light: How Ultraviolet Disinfection Can Prevent the Nosocomial Transmission of COVID-19 and Other Infectious Diseases. *Appl. Microbiol.* **2021**, *1*, 537–556.
- (16) Escombe, A. R.; Moore, D. A. J.; Gilman, R. H.; Navincopa, M.; Ticona, E.; Mitchell, B.; Noakes, C.; Martinez, C.; Sheen, P.; Ramirez, R.; Quino, W.; Gonzalez, A.; Friedland, J. S.; Evans, C. A. Upper-Room Ultraviolet Light and Negative Air Ionization to Prevent Tuberculosis Transmission. *Plos Med.* **2009**, *6*, No. e43.
- (17) Fischer, R.; Morris, D.; van Doremalen, N.; Sarchette, S.; Matson, M. J.; Bushmaker, T.; Yinda, C. K.; Seifert, S.; Gamble, A.; Williamson, B.; Judson, S.; de Wit, E.; Lloyd-Smith, J.; Munster, V.

Effectiveness of N95 Respirator Decontamination and Reuse against SARS-CoV-2 Virus. *Emerg. Infect. Dis. J.* **2020**, *26*, 2253.

(18) Storm, N.; McKay, L. G. A.; Downs, S. N.; Johnson, R. I.; Birru, D.; de Samber, M.; Willaert, W.; Cennini, G.; Griffiths, A. Rapid and complete inactivation of SARS-CoV-2 by ultraviolet-C irradiation. *Sci. Rep.* **2020**, *10*, 22421.

(19) Ruetalo, N.; Businger, R.; Schindler, M. Rapid, dose-dependent and efficient inactivation of surface dried SARS-CoV-2 by 254 nm UV-C irradiation. *Eurosurveillance* **2021**, *26*, 42.

(20) Ma, B.; Linden, Y. S.; Gundy, P. M.; Gerba, C. P.; Sobsey, M. D.; Linden, K. G. Inactivation of Coronaviruses and Phage Phi6 from Irradiation across UVC Wavelengths. *Environ. Sci. Technol. Lett.* **2021**, *8*, 425–430.

(21) Ueki, H.; Ito, M.; Furusawa, Y.; Yamayoshi, S.; Inoue, S.-I.; Kawaoka, Y.; Bouvier, N. M. A 265-Nanometer High-Power Deep-UV Light-Emitting Diode Rapidly Inactivates SARS-CoV-2 Aerosols. *mSphere* **2022**, *7*, No. e0094121.

(22) Fischer, R. J.; van Doremalen, N.; Adney, D. R.; Yinda, C. K.; Port, J. R.; Holbrook, M. G.; Schulz, J. E.; Williamson, B. N.; Thomas, T.; Barbian, K.; Anzick, S. L.; Ricklefs, S.; Smith, B. J.; Long, D.; Martens, C.; Saturday, G.; de Wit, E.; Gilbert, S. C.; Lambe, T.; Munster, V. J. ChAdOx1 nCoV-19 (AZD1222) protects Syrian hamsters against SARS-CoV-2 B.1.351 and B.1.1.7. *Nat. Commun.* **2021**, *12*, 5868.

(23) van Doremalen, N.; Bushmaker, T.; Morris, D. H.; Holbrook, M. G.; Gamble, A.; Williamson, B. N.; Tamin, A.; Harcourt, J. L.; Thornburg, N. J.; Gerber, S. I.; Lloyd-Smith, J. O.; de Wit, E.; Munster, V. J. Aerosol and Surface Stability of SARS-CoV-2 as Compared with SARS-CoV-1. *N. Engl. J. Med.* **2020**, *382*, 1564–1567.

(24) Bourouiba, L. Fluid Dynamics of Respiratory Infectious Diseases. In *Annual Review of Biomedical Engineering*; Yarmush, M. L., Ed.; Annual Review, 2021; Vol. 23, pp 547–577.

(25) Bourouiba, L. The Fluid Dynamics of Disease Transmission. In *Annual Review of Fluid Mechanics*; Moin, P.; Stone, H. A., Eds.; Annual Review, 2021; Vol. 53, pp 473–508.

(26) Bowen, R. A.; Gilgunn, P.; Hartwig, A. E.; Mullen, J. Prevention of Airborne Transmission of SARS-CoV-2 by UV-C Illumination of Airflow. *COVID* **2021**, *1*, 602–607.

(27) Xu, P.; Peccia, J.; Fabian, P.; Martyny, J. W.; Fennelly, K. P.; Hernandez, M.; Miller, S. L. Efficacy of ultraviolet germicidal irradiation of upper-room air in inactivating airborne bacterial spores and mycobacteria in full-scale studies. *Atmos. Environ.* **2003**, *37*, 405–419.

(28) Ethington, T.; Newsome, S.; Waugh, J.; Lee, L. D. Cleaning the air with ultraviolet germicidal irradiation lessened contact infections in a long-term acute care hospital. *Am. J. Infect. Control* **2018**, *46*, 482–486.

(29) Qiao, Y. C.; Yang, M.; Marabella, I. A.; McGee, D. A. J.; Aboubakar, H.; Goyal, S.; Hogan, C. J.; Olson, B. A.; Torremorell, M. Greater than 3-Log Reduction in Viable Coronavirus Aerosol Concentration in Ducted Ultraviolet-C (UV-C) Systems. *Environ. Sci. Technol.* **2021**, *55*, 4174–4182.

(30) Nardell, E. A. Air Disinfection for Airborne Infection Control with a Focus on COVID-19: Why Germicidal UV is Essential- (dagger). *Photochem. Photobiol.* **2021**, *97*, 493–497.

(31) Nardell, E. A.; Nathavitharana, R. R. Airborne Spread of SARS-CoV-2 and a Potential Role for Air Disinfection. *JAMA* **2020**, *324*, 141–142.

(32) First, M.; Rudnick, S. N.; Banahan, K. F.; Vincent, R. L.; Brickner, P. W. Fundamental factors affecting upper-room ultraviolet germicidal irradiation – part I. Experimental. *J. Occup. Environ. Hyg.* **2007**, *4*, 321–331.

(33) Beggs, C. B.; Avital, E. J. Upper-room ultraviolet air disinfection might help to reduce COVID-19 transmission in buildings: a feasibility study. *PeerJ* **2020**, *8*, No. e10196.

(34) McDevitt, J. J.; Milton, D. K.; Rudnick, S. N.; First, M. W. Inactivation of Poxviruses by Upper-Room UVC Light in a Simulated Hospital Room Environment. *PLoS One* **2008**, *3*, No. e3186.